Maskless Lithography Using Patterned Amorphous Silicon Layer Induced by Femtosecond Laser Irradiation

Amirkianoosh Kiani*, Krishnan Venkatakrishnan* and Bo Tan**

*Department of Mechanical and Industrial Engineering, Ryerson University,
350 Victoria Street, Toronto, ON, Canada M5B 2K3, akkiani@ryerson.ca
**Department of Aerospace Engineering, Ryerson University,
350 Victoria Street, Toronto, ON, Canada M5B 2K3

ABSTRACT

In this research, we reported a maskless lithography method by a combination of laser amorphization of silicon and wet alkaline etching. This technique can lead to a promising solution for maskless lithography because in comparison to the previous techniques, it involves less processing steps and requires simple equipment configuration. Scanning Electron Microscope (SEM), a Micro-Raman and Energy Dispersive X-ray (EDX) spectroscopy analyses were used to evaluate the quality of amorphous layer and the etching process.

Keywords: maskless lithography, amorphous silicon, femtosecond laser

1 INTRODUCTION

Photolithography is considered to be an important technique to fabricate microelectromechanical and nanoelectromechanical systems (MEMS and NEMS) and Lab-on-a-Chip systems [1,2]. In this technique, a photomask is required for replication, and the fabrication of photo masks is an expensive process and time consuming, because there are several steps involved in the process of its fabrication [3-5]. In recent years, numerous attempts have been proposed for maskless lithography technique such as electron beam lithography (EB) [6], focused ion-beam (FIB) lithography [7], scanning-probe microscopy (SPM) and Tribo Nano Lithography (TNL) based on atomic force microscope (AFM) [8-11]. Although, these techniques have some advantages, they entail time consuming processing steps and employ complex and expensive equipments and systems which require well-trained user for their operation, leading to high operating cost.

In this research, we reported a maskless lithography method by a combination of laser amorphization of silicon and wet alkaline etching. This technique can lead to a promising solution for maskless lithography since it involves less processing steps and requires simple equipment configuration. In comparison to systems such as AFM, FIB and Electron Beam, which are employed in other techniques, lasers are much more economical and can be acquired and operated at lower cost [12] which makes it particularly suitable for rapid prototyping and custom-scale manufacturing for a wide variety of applications in MEMS, NEMS, fabrication of semiconductor and Lab On a Chip systems.

2 EXPERIMENTAL SETUP AND FABRICATION PROCESS

To study the silicon amorphization, un-doped <100> oriented silicon wafers were used. Prior to laser irradiation, we cleaned the samples with alcohol and ultra pure water. As shown in Fig. 1, silicon wafers were irradiated with femtosecond pulses with pulse energy well below the damage threshold. Finally, the treated samples were etched in a KOH solution.The Femtosecond laser used in the study was a diode-pumped, Yb-doped system with the average output power of 11 W and a central wavelength of 1030 nm. The range of pulse frequency is between 200 kHz and 26 MHz. This laser emits pulses of 200 fs pulse duration. The theoretical focused laser spot diameter (d_0) is calculated to be 10.38 µm from: $d_o \approx 1.27\ \lambda_o F/D$. [13]

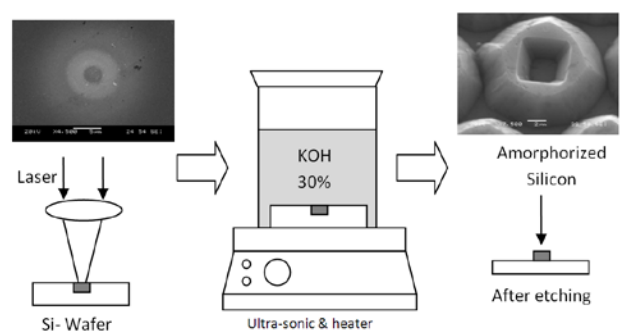

Figure 1. Process of experiment

3 RESULTS AND DISCUSSION

Figure 2 shows morphology of irradiated samples during etching process with alkaline etchant (KOH 30%, temperature: 80º C). After etching, it was observed that the non-irradiated area and the central region of the laser irradiated zone were etched by alkaline etchant; whereas, the annulus around the central region of the laser spot was not etched. Consequently, a ring feature stood out on the silicon substrate, suggesting that the amorphous layer resists to KOH. This etch ratio value agrees well with the

result of etch rate of amorphous silicon reported by Kawasegi *et al*.[11,14,15] According to their reports, the etch rate of amorphous silicon which generated by magnetron spattering is about 30 times lower than the etch rate of crystalline silicon<100>.

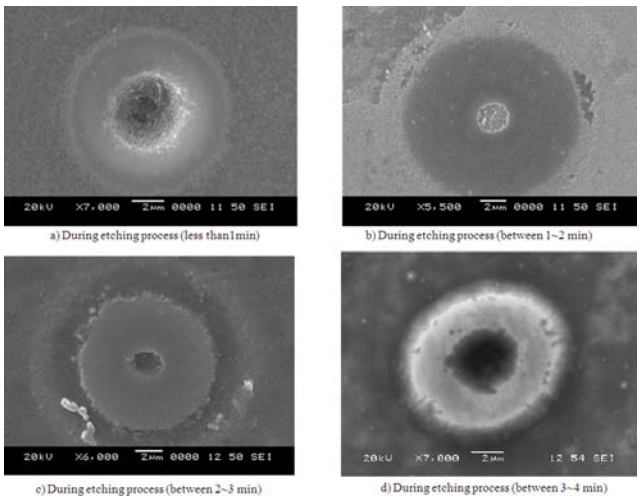

Figure 2. SEM images of irradiated samples during etching process.

Because of the Gaussian distribution of the beam the laser fluence at the center region was above the surface damage threshold, therefore, ablation occurred in this area. It was observed that after etching the center zone was removed by etchant. Thus, the central zone was not in amorphous state. However, in the surrounding annulus area, the amorphous phase was formed on crystalline silicon which acted as an etch stop during etching process.

In order to obtain a smaller circular dot instead of a donut feature, the laser beam should be accurately controlled such that central peak of the Gaussian beam intensity does not exceed the surface damege threshold. Figure 3 shows SEM image of circular feature obtained after wet etching.

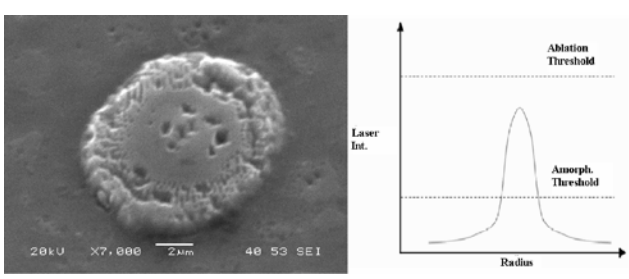

Figure 3. SEM image of feature after 3 min etching - solid round at 0.2J/cm^2

Figure 4 presents a line feature with 1.4 µm thickness and 6 µm width generated with a scanning laser spot of 0.28 J/cm^2 at 26 MHz. As it is shown in Figure 4, the irradiated zone was not etched; however, the non-irradiated area was dissolved during etching and finally, a pyramid-like structure was formed on silicon substrate. The etched (100) planes have a slope with an angle of 54.7º as expected. [16]

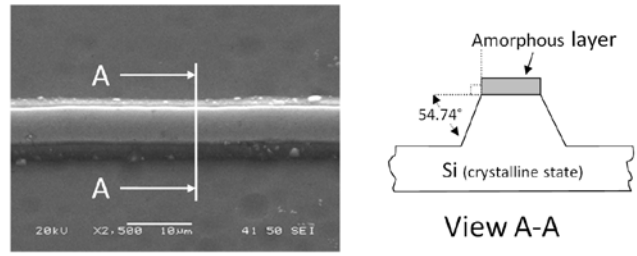

Figure 4. SEM image at the incident angle of 35° of line feature after etching in KOH (Pulse energy: 0.28 J/cm^2)

In order to investigate the relationship between the effects of laser parameters and resulting silicon amorphorized layer properties induced by high repetition femtosecond laser pulses, various laser parameters such as pulse frequency and pulse number were applied to study the effects of the parameters in the amorphization process.

As shown in Figure 5, the amorphorized layers generated respectively at 8, 13 and 26 MHz had a better quality and repeatability at higher pulse frequency (at 26 MHz). It is due to this fact that with higher pulse frequency at 26 MHz, the fluctuations in laser power is less in comparison with the power fluctuation at 8 and 13 MHz [17]. In actuality, the silicon amorphization needs a strict parameters control and the higher power fluctuation in lower pulse frequencies (at 8 and 13 MHz), may result in ablation or poor quality of amorphorized layer.

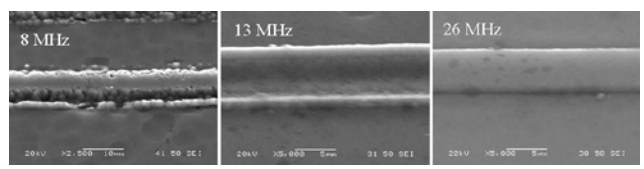

Figure 5. SEM images at different pulse repetition rates (pulse duration: 214 fs).

As shown in Fig. 6, it was observed that amorphorized zones became wider with the number of pulses increasing. The increase of number of pulses results in increasing the number of photons per unit volume which induced multi-photon ionization, thus more energy is injected into the Si-surface, so the heat affected areas would expand [18].

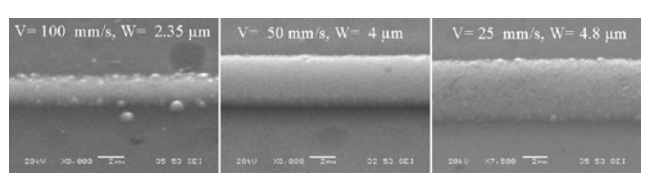

Figure 6. SEM images of silicon samples after irradiated with 214 fs laser (26 MHz) at different number of pulses.

Corresponding to 100, 50 and 25 mm/s, the numbers of pulses incidence at the focal points at 26 MHz and power of 7.2W, are 2675, 5356 and 1072, respectively. Fig. 7 shows

the width of the amorphorized zone enlarged with the incident pulse number increasing. However, from the experimental results it can be concluded that by increasing the pulse number, the increasing of amorphization width nearly reaches saturation.

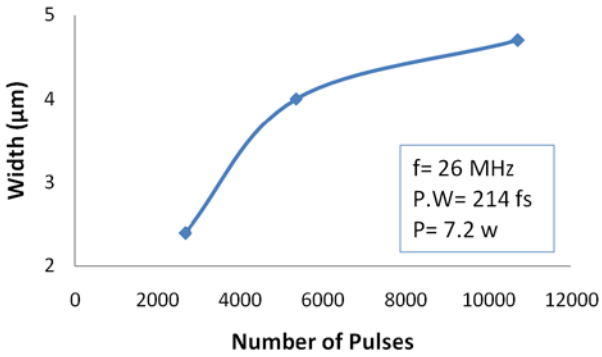

Figure 7. Width of amorphorized zone vs. number of pulses.

Figure 8 presents the smallest lines generated with reducing the pulse energy to 0.1 J/cm^2 at the frequency of 26 MHz. The line width obtained with the 10 µm laser spot is around 150 nm which is around 1/67 of the laser spot diameter. Using the same technique, sub-100 nm ablated features generated with a laser spot of 2 µm diameter was reported in previous research work [3].

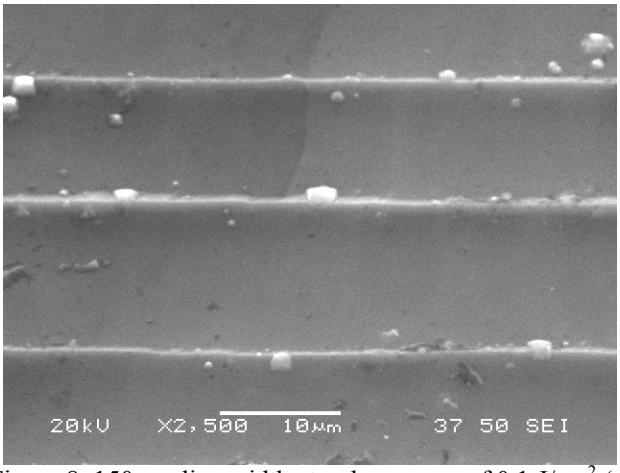

Figure 8. 150 nm line width at pulse energy of 0.1 J/cm^2 (at 26 MHz)

In order to investigate the chemical and structural properties of generated layer by femtosecond laser pulses on silicon substrate, a Micro-Raman and Energy Dispersive X-ray (EDX) spectroscopy analyses were hired.

EDX analysis of the irradiated zone excluded the possibility of compound formation, thus, a generated layer on the top surface has not been converted to a chemical compound, such as silicon oxide and silicon hydroxide. (Fig. 9)

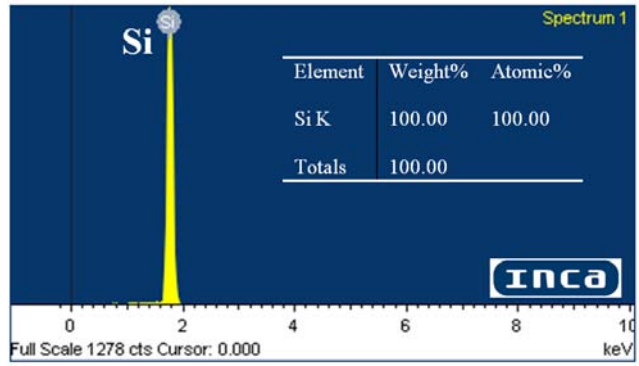

Figure 9. EDX analysis of irradiated zone.

Raman Spectroscopy analyses of different zones after laser irradiation showed a sharp peak at the wavenumber of 517 cm^{-1}, which is the characteristic peak of crystalline silicon. Also, another peak was observed at the wavenumber of 506.9 cm^{-1} which is the characteristic of amorphous silicon [19] (See Fig. 10). Therefore, it can be concluded that the irradiated zone was converted from crystalline silicon into amorphous silicon.

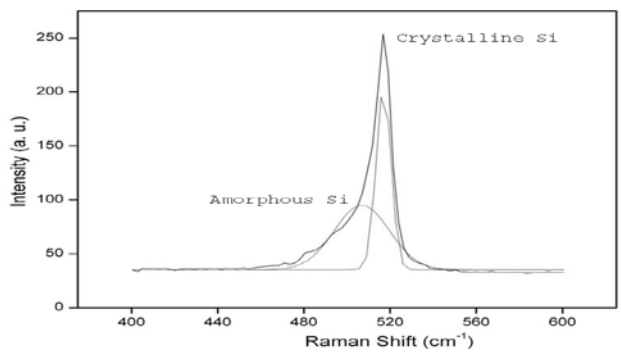

Figure 10. Raman spectroscopy graph.

4 CONCLUSION

In this study, we proposed a new method for maskless lithography, using a combination of laser amorphization of silicon and wet chemical etching. Formed amorphous layers acted as an etch stop in alkaline etchant and micro and sub-micro features were fabricated on silicon substrate. Using high frequency (MHz) femtosecond pulses laser makes this technique suitable for rapid prototyping and custom-scale manufacturing for a wide variety of applications in MEMS, NEMS, fabrication of semiconductor and Lab On a Chip systems which demand for flexibility in re-design. It was found that higher frequency rate of laser pulses gives smooth morphology with better repeatability. Increasing number of pulses was seen to increase the line width. Also, by reducing the pulse energy, features less than 1/64 the focused spot size were generated. Submicron and nano scale feature size can be expected by optimizing etching and laser parameters. Scanning Electron Microscope (SEM), a Micro-Raman and Energy Dispersive X-ray (EDX) spectroscopy were used to study the quality of

generated amorphous layer. In the future, more investigations will be carried out to reduce the features size in nano-scale by optimizing laser parameters and etching process.

REFERENCES

[1] D. Bauerle, "*Laser processing and chemistry*", 3rd ed.; Springer: New York, 2000.

[2] D. Lim, Y. Kamotani, B. Cho, J. Mazumder, S. Takayama; *Lab Chip.* **3**, 318-323, 2003.

[3] B. Tan, A. Dalili, K. Venkatakrishnan, *Appl. Phys. A.* **95**, 537-545, 2009.

[4] P. Stanley, K. Venkatakrishnan, L. E. N. Lim, *Vac. Sci. Technol. B.* **21**, 204-206, 2003.

[5] K. Venkatakrishnan, B. K. A. Ngoi, P. Stanley, L.E.N. Lim, B. Tan, N. R. Sivakumar, *Appl. Phys. A.* **74**, 493-496, 2002.

[6] H. Yasuda, S. Arai, J. Kai, Y. Ooae, T. Abe, S. Maruyama, T. Kiuchi, *J. Vac. Sci. Technol.* B. **14,** 3813–3820, 1996.

[7] B. Schmidt, L. Bischoff, J. Teichert, *Sensors Actuators A*. **61,** 369–373, 1997.

[8] F. S. S. Chien, C. L. Wu, Y. C. Chou, T. T. Chen, S. Gwo, W. F. Hsieh, *Appl. Phys. Lett.* **75,** 2429–2431, 1999.

[9] Y. Y. Zhang, J. Zhang, G. Luo, X. Zhou, G. Y. Xie, T. Zhu, Z. F. Liu, *Nanotechnology.* **16**, 422–842, 2005.

[10] D. A. Weinberger, S. Hong, C. A. Mirkin, B. W. Wessels, T. B. Higgins, *Adv. Mater.* **12,** 1600–1603, 2000.

[11] N. Kawasegi, N. Morita, S. Yamada, N. Takano, T. Oyama, K. Ashida, *J. Nanotechnology*. **16**, 1411-1414, 2005.

[12] K. Venkatakrishnan, B. Tan, *J. Micromech. Microeng.* **16**, 1587-1592, 2006.

[13] K. Venkatakrishnan, B. Tan, P. Stanely, L.E.N. Lim, B.K.A. Ngoi, *J. Opt. Eng.* **41**, 1441-1445, 2002.

[14] N. Kawasegi , N. Morita, S. Yamada , N. Takano, T. Oyama, S. Momota, J. Taniguchi, I. Miyamoto, *Appl. Surf. Sci.* **253**, 3284-3291, 2007.

[15] J.W. Park, N. Kawasegi, N. Morita, D. W. Lee, *App Phys Lett.* **85(10)**, 1766-1768, 2004.

[16] M. J. Archer, F. S. Ligler, *Sensors*. **8**, 3848-3872, 2008.

[17] A. Kiani, K. Venkatakrishnan, B. Tan, *Optics Express* **18** (3), 1872-1878, 2010.

[18] N. H. Ma, H.L. Ma, M. J. Zhong, J.Y. Yang,Y. Dai, G. Ye, Z. Y. Yue, G. H. Ma, J. R. Qiu, *Materials Lett.* **63**(1), 151-153, 2009.

[19] J. Bonse, K. W. Brzezinka, A. J. Meixner, *Appl. Surf. Sci.* **221**, 215-230, 2004.